

# Emergence and approximation of tori

Taoufik Bakri and Ferdinand Verhulst  
Mathematisch Instituut, University of Utrecht  
PO Box 80.010, 3508 TA Utrecht  
The Netherlands  
email: f.verhulst@uu.nl

April 6, 2023

## Abstract

We will consider isolated quasi-periodic solutions and families of quasi-periodic solutions. A remarkable aspect of the system Sprott A and a few generalisations is the observed presence of families of quasi-periodic solutions organised on invariant tori, a phenomenon known earlier in the context of conservative systems and the so-called KAM-theorem. In addition we link the tori bifurcation phenomenon in dissipative systems to time-reversal and canards. For more general isolated tori in dissipative systems we can develop an integral iteration scheme based on contraction and quasi-periodic secularity conditions. The technique leads to conditions for the presence of quasi-periodic solutions and possibly invariant manifolds. The general idea can be illustrated by for instance coupled Van der Pol-equations and other coupled oscillators.

To study applications in mechanics and other fields, in general in dynamical systems, it is useful to focus on basic ingredients of the systems. One considers for instance periodic solutions, integral manifolds, chaos, energy exchange of oscillators and many other phenomena. We will pay attention to quasi-periodic solutions that can be isolated or are organised on a torus.

## 1 Quasi-periodicity in dissipative systems

A number of chaotic 3-dimensional systems, in fact 17 autonomous systems with linear and quadratic terms only and one parameter ( $a$ ), have been listed and studied in [10], see also [20]; all these systems are dissipative, i.e. the 3-dimensional phase-flow is not volume-preserving. The systems are numbered NE1, ..., NE17 with one of them, called Sprott A (or NE1). The study of these 17 systems is very instructive as 3-dimensional systems generally show much more complexity in bifurcations and chaos than 2-dimensional

ones and as the 17 systems are relatively simple, quadratic and with one parameter. The evidence for chaos in [10] is mainly numerical but it is an important start. Strong evidence in [16] and [17] has shown that in the Sprott A system families of tori arise. It has been demonstrated in [8] that these families are caused by certain symmetry characteristics of the system.

## 1.1 The Sprott A system

A remarkable aspect of the systems Sprott A and NE9 is the observed presence of families of invariant tori, known in conservative systems but it is remarkable that we have here dissipative systems with a small parameter. This aspect was studied in more detail for Sprott A in [16] and [17] who correctly observe that we have a kind of KAM tori, see for KAM-theory [1]; the evidence is numerical.

A novel result in [8] is that we can complete the theoretical picture both for Sprott A and NE9 by linking the tori bifurcation phenomenon to time-reversal and canards. In addition, for both systems we can identify a number of periodic solutions on the tori. Lazar's frequency condition [14] can be used to demonstrate the process of chaos between the tori.

For the Sprott A system unbounded solutions can only be found on the  $z$ -axis. Another novel aspect is that for system NE9 this is different; we find in [8] 'rings' of initial values leading to unbounded solutions. Scaling near infinity and using again geometric singular perturbation theory provides insight in this dynamics.

We formulate the equations for the system Sprott A:

$$\dot{x} = y, \dot{y} = -x - yz, \dot{z} = y^2 - a, \quad (1)$$

with parameter  $a > 0$ . The Sprott A system is a special case of the Nosé-Hoover oscillator. It was shown in [8] that in this dissipative system an infinite number of tori are present that is caused by symmetries of the system. It is discussed with other physical examples in [18], see for the theory also [9] and [13].

## 1.2 An intermezzo on canards

Symmetries are an essential ingredient of understanding the dynamics of the Sprott A system. Another interesting aspect is the presence of slow-fast systems that arise for certain values of the parameter and for certain initial values. In the Sprott A system this involves the presence of canards that complicate the dynamics of quasi-periodic solutions. We give a short description of the canard phenomenon, see for an extensive discussion and references [25]. In general canards may be present in slow-fast systems of the form

$$\dot{x} = f(x, y), \varepsilon \dot{y} = g(x, y).$$

The dynamics of  $x(t)$  will in general be relatively slow with respect to the dynamics of  $y(t)$  as  $\dot{y}$  will be proportional to  $1/\varepsilon$ . However, this will not be true in a neighbourhood of

space where  $g(x, y) = 0$ . Suppose that we can solve the equation  $g(x, y) = 0$  that can be an algebraic or transcendental equation or a set of such equations (as we did not specify the dimensions of  $x$  and  $y$ ).

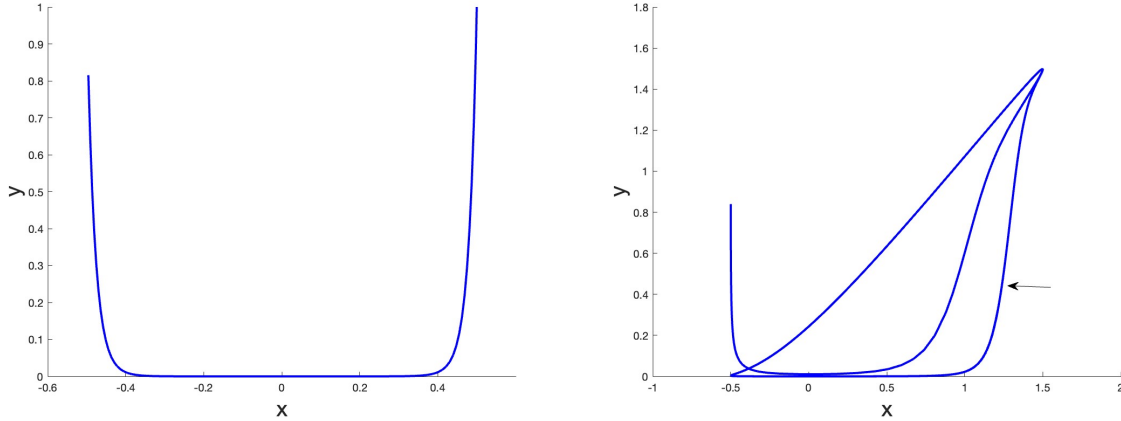


Figure 1: Left, the canard behaviour demonstrated for eq. (2),  $\varepsilon = 0.01$ . Right, a solution with canards of eq. (3) where the solution tends to a periodic solution.

Suppose the solution is  $y = y(x)$  that represents a curve or more general a manifold in  $x, y$ -space. We will call this a slow manifold as the dynamics on or near this manifold will have a time-behaviour comparable to that of the  $x(t)$  component. To understand the canard phenomenon 2 elements are important. First, that the slow manifold may be stable for a finite interval of time; it has been shown in [25] that in this case the solutions in a neighbourhood of the slow manifold will become exponentially close proportionally to  $e^{-ct/\varepsilon}$  with  $c$  a positive constant dependent on the system. If at some point the slow manifold changes stability, it takes some time to leave the slow manifold because of the extreme exponential closeness. We call this delay of instability and the dynamical phenomenon a “canard”. An illustration by a simple example is given in fig. 1 (left). The equation used here is:

$$\dot{x} = 1, \varepsilon \dot{y} = xy. \quad (2)$$

We start at  $x(0) = -0.5, y(0) = 0.83$ . As we took  $\varepsilon = 0.01$  the initial  $\dot{y}(0)$  will be  $-83$  and  $y(t)$  will move quickly to the  $x$ -axis. We can solve the problem explicitly producing:

$$x(t) = x(0) + t, y(t) = y(0)e^{\frac{t}{\varepsilon}(x(0)+t)}.$$

Starting with  $x(0)$  negative and  $y(0)$  positive the  $x$ -axis will be the approximate slow manifold. The exponential attraction with timelike variable  $t/\varepsilon$  has as a consequence that the solution approaches the  $x$ -axis exponentially close as long as  $x(0) \leq t \leq \delta < 0$  with  $\delta$  a positive constant. It was shown in [25] that this exponential closeness is a general feature of stable slow manifolds in slow-fast systems. The solution  $x(t)$  passes zero after which the

slow manifold becomes unstable. However, this instability is delayed because the solution has become extremely close to the slow manifold in its stable stage. This causes the canard behaviour.

A slightly more complicated system where the solutions remain bounded and tend to a periodic solution with a canard is the 2-dimensional system:

$$\dot{x} = \sin(t), \quad \varepsilon \dot{y} = xy - y^2. \quad (3)$$

We choose again  $x(0) = -0.5, y(0) = 0.83$ . In this case we have 2 slow manifolds that intersect:  $y = 0$  and  $y = x$ . We have again canard behaviour when the solutions follow the  $x$ -axis (approximate slow manifold) and passes  $x = 0$ . The slow manifold  $y = x$  becomes stable and the solutions return following  $y = x$ . The solutions approach the closed curve indicated by an arrow.

### 1.3 Dissipative Sprott B system

Consider the system:

$$\dot{x} = y, \quad \dot{y} = -x - yz, \quad \dot{z} = Ax^2 + By^2 - a, \quad (4)$$

with  $a > 0$ .  $A, B$  are fixed constants. It turns out that near the origin of phase-space one parameter,  $A + B$ , plays an essential part. We call system (4) system Sprott B, it reduces to the Sprott A system if  $A = 0, B = 1$ . For reasons of comparison we will choose:

$$A + B = 1.$$

As for the Sprott A system we have that for arbitrary  $a$  the  $z$ -axis is an invariant manifold with unbounded solutions  $x = y = 0, z(t) = z(0) - at$ .

An interesting discrete symmetry feature of (1) was formulated in [7]. It also holds for the Sprott B system (4):

#### Discrete symmetry

*If  $(x(t), y(t), z(t))$  is a solution of system (4) then also  $(-x(t), -y(t), z(t))$  is a solution.*

This is verified by substitution. An important feature involving time reversal of (4) is:

#### Time-reversal of Sprott B

*If  $(x(t), y(t), z(t))$  is a solution of system (4) then by putting  $\bar{x} = x, \bar{y} = -y, \bar{z} = -z$  and reversing time  $\tau = -t$  then  $(\bar{x}(\tau), \bar{y}(\tau), \bar{z}(\tau))$  is a solution.*

Such time-reversal symmetry is called  $R$ -symmetry in [13].

Note that by differentiating the equation for  $x$  we can rewrite system (4) as:

$$\ddot{x} + \dot{x}z + x = 0, \quad \dot{z} = Ax^2 + B\dot{x}^2 - a. \quad (5)$$

In the sequel we will assume  $0 < a \ll 1$ .

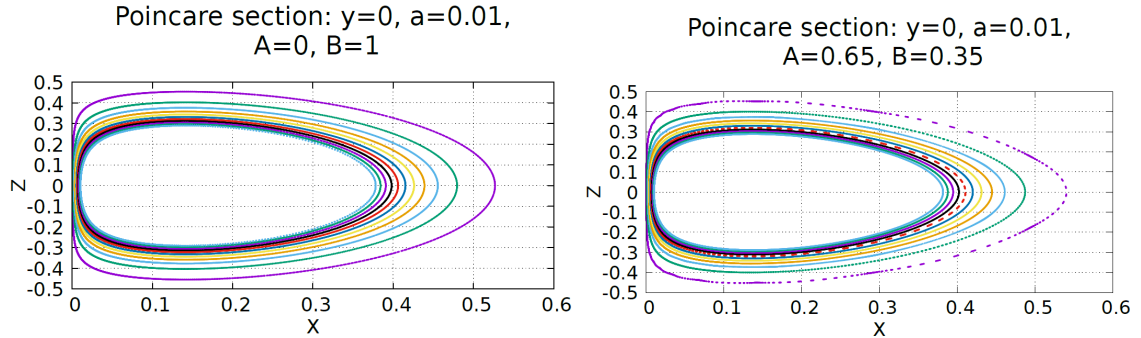


Figure 2: Poincaré map in the plane  $y = 0$  of the Sprott A system (1) (left,  $A = 0, B = 1$ ) and the Sprott B system (4) (right,  $A = 0.65, B = 0.35$ ) near the origin of phase-space for  $a = 0.01$ . The behaviour near the  $z$ -axis shows canard behaviour for various initial conditions.

#### 1.4 A periodic solution near the origin

Considering small values of parameter  $a$  and solutions  $\varepsilon$ -close to the origin of phase-space we transform:

$$x \rightarrow \varepsilon x, y \rightarrow \varepsilon y, z \rightarrow \varepsilon z, a = \varepsilon^2 a_0. \quad (6)$$

with  $a_0 > 0$  and  $\varepsilon$  a small positive parameter. System (4) becomes:

$$\dot{x} = y, \dot{y} = -x - \varepsilon y z, \dot{z} = \varepsilon (A x^2 + B y^2 - a_0). \quad (7)$$

Transforming  $(x, y) \mapsto (r, \phi)$  we use amplitude-phase coordinates  $x = r \cos(t + \phi), y = -r \sin(t + \phi)$  and average over time  $t$ . For the theory of averaging see [19]; we find to first order in  $\varepsilon$ :

$$\dot{r} = -\frac{\varepsilon}{2} r z, \dot{\phi} = 0, \dot{z} = \frac{\varepsilon}{2} (A r^2 + B r^2 - 2a_0). \quad (8)$$

From the second Bogoliubov theorem (see [24]) we know that a critical point of system (8) under certain implicit function conditions corresponds with a periodic solution of system (7) that is  $\varepsilon$ -close to the critical point. We find for the critical point:

$$r_c = \sqrt{\frac{2a_0}{A+B}} = \sqrt{2a_0}, \quad z = 0. \quad (9)$$

If the Jacobian of the averaged system at the critical point is structurally stable the stability of the periodic solution follows from the eigenvalues at the critical point. However, the eigenvalues are given by the characteristic equation:

$$\lambda(\lambda^2 + a_0) = 0.$$

For autonomous equations we will always find one eigenvalue zero but the other two are purely imaginary, we have existence of a periodic solution but its stability is not clear at

this stage. We apply second order averaging, see [19] for the procedure, but we find after some calculations again purely imaginary eigenvalues of the critical point. We conclude to Lyapunov stability of the periodic solution to second order in  $\varepsilon$ .

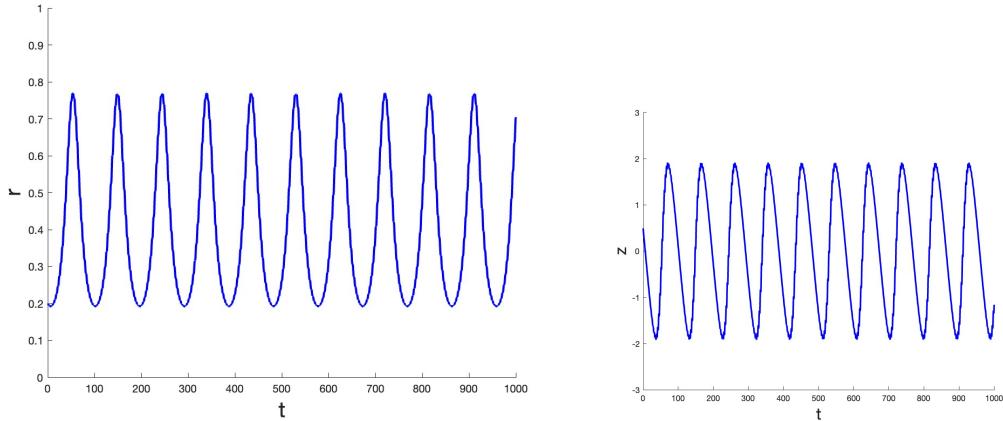


Figure 3: Behaviour of  $r(t)$ ,  $z(t)$  of the Sprott B system (4),  $A = 1, B = 0$  near the periodic solution close to the origin of phase-space;  $a = 0.1, \varepsilon = 0.05, z(0) = 0.5, x(0) = 0.2, y(0) = 0$ ,  $z(t)$  alternates in sign.

Returning to the Sprott A system we have  $A = 0, B = 1$ . The averaged system (8) shows exactly the same behaviour as the averaged system for Sprott A putting  $A + B = 1$ . With the same scaling we have close to the periodic solution the same dynamical behaviour for the Sprott A and Sprott B system. The periodic solution found by averaging both for the Sprott A and Sprott B systems serve as *organising centre* for families of tori. Different behaviour arises when  $z(t)$  starts outside this region and becomes small. We demonstrate the behaviour near the periodic solution numerically for system (7) in fig. 3. Choosing  $A = 0.5, B = 0.5$  gives similar behaviour.

## 2 Canard behaviour near the $z$ -axis

It was shown in [7] that if  $a$  is small we have a singular perturbation problem with canard behaviour for the Sprott A system (1). We study the Sprott B system (4) as a slow-fast system and will apply Tikhonov's theorem [21]. Note that for system (4)

$$\frac{dr^2}{dt} = -2\dot{x}^2 z,$$

so, as for the Sprott A system and as long as  $z(t)$  is positive the  $(x, y)$  phase-flow is strongly damped; if  $z(t)$  is negative, the flow is excited. We expect that when starting with positive  $z(0)$  large enough the solution tends relatively fast to a neighbourhood of

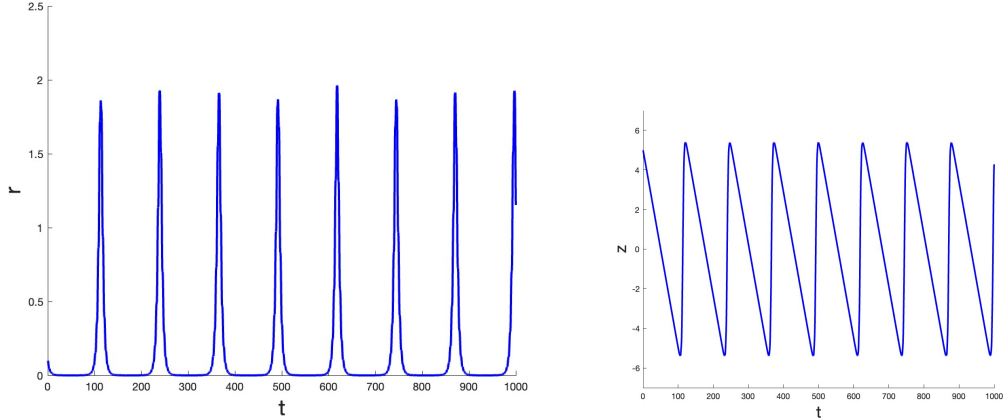


Figure 4: Canard behaviour of  $r(t), z(t)$  of the Sprott B system (10),  $A = 0.5, B = 0.5$ . We have  $a = 0.1, \varepsilon = 0.1, z(0) = 5, x(0) = 0.1, y(0) = 0$ ,  $z(t)$  alternates in sign. The value of  $z(0)$  forces the  $x(t), y(t)$  behaviour to approach the  $z$ -axis in its stable part, when passing the origin this part of the  $z$ -axis becomes unstable but the motion along the axis persists for some time (canard behaviour).

$x(t), y(t) = O(\sqrt{\varepsilon})$  (near the  $z$ -axis); after this the canard behaviour near the  $z$ -axis will start, see fig. 4.

To put the system in the formulation of Tikhonov's theorem we rescale system (4) slightly differently:

$$x = \varepsilon \bar{x}, y = \varepsilon \bar{y}, a = \varepsilon a_0.$$

Omitting the bars system (4) becomes:

$$\dot{x} = y, \dot{y} = -x - yz, \dot{z} = -\varepsilon a_0 + \varepsilon^2(Ax^2 + By^2), A + B = 1. \quad (10)$$

Rescaling time  $\tau = \varepsilon t$  we find the equivalent system:

$$\varepsilon \frac{dx}{d\tau} = y, \varepsilon \frac{dy}{d\tau} = -x - yz, \frac{dz}{d\tau} = -a_0 + \varepsilon(Ax^2 + By^2). \quad (11)$$

According to geometric singular perturbation theory, system (11) shows fast motion of the  $x, y$ -component in the timelike variable  $\tau$ , except in an  $O(\varepsilon)$  neighbourhood of the 1-dimensional approximate slow (or critical) manifold  $M_0$  defined by:

$$y = 0, -x - yz = 0. \quad (12)$$

The approximate slow manifold  $M_0$  corresponds with the  $z$ -axis in 3-dimensional phase-space, it is normally hyperbolic when excluding a neighbourhood of  $z = 0$  as we have for the fast part of the system that the real part of the spectrum is  $-z/2$ .  $M_0$  approximates the smooth slow manifold  $M_\varepsilon$  that exists for solutions of system (11). According to section

15.7 of [25], when excluding a neighbourhood of  $z = 0$ ,  $M_0$  approximates  $M_\varepsilon$  exponentially close. To fix ideas we take initially  $x(0), y(0)$  small and  $z(0) > 0$ .

When starting outside  $M_0$  at positive  $z(0) = z_0$ ,  $z(t)$  of system (11) will change little. An  $O(\varepsilon)$  approximation of the fast solutions of the system will be of the form:

$$X_0(t) = x_0 e^{-z_0 t/2} \cos\left(\sqrt{4 - z_0^2} \frac{t}{2}\right). \quad (13)$$

The approximation is valid on an interval  $O(1)$  in  $\tau$ ,  $O(1/\varepsilon)$  in  $t$  as long as we do not enter a  $\varepsilon$ -neighbourhood of  $M_0$ . From (13) we can estimate the fast time  $T_1$  needed to approach  $M_0$ :

$$x(0) e^{-z_0 T_1/2} \cos\left(\sqrt{4 - z_0^2} \frac{T_1}{2}\right) = \varepsilon. \quad (14)$$

Ignoring the oscillations a rough estimate is

$$T_1 \approx -\frac{2}{z_0} \ln\left(\frac{\varepsilon}{x_0}\right). \quad (15)$$

The approximate time needed for the motion until  $z = 0$  along  $M_0$  is  $T_2 = z_0/(\varepsilon a_0)$ . Using the R-symmetry for system (4) (subsection 1.3) we find the estimate of the return time  $T \geq 2(T_1 + T_2)$  of the flow. The pulse-like behaviour for the fast motion of the flow is shown in fig. 4. The solutions of the slow-fast system will traverse an  $O(\sqrt{\varepsilon})$  neighbourhood of the origin spending the same time for positive and negative values of  $z$ .

Geometric singular perturbation theory in combination with time reversal and symmetry produces the behaviour shown in the Poincaré maps of fig. 2. Increasing  $\varepsilon$  we expect the tori to break up, maybe with Cantor gaps as in near-integrable Hamiltonian systems. In [7] it was shown by the SDDS NAFF algorithm of [14] that in the tori region we can locate an accumulation of frequencies of the quasi-periodic and periodic solutions on the tori producing loss of regularity of the frequency map. This is carried out by looking for quasi-periodic and periodic solutions on the tori and identifying by Fourier analysis the relevant periods of the solutions. After constructing the frequency map, this yields chaotic motion between the tori. The analysis carries over to the Sprott B system.

### 3 Interaction of self-excited and parametric excitation

Consider a modification of the system formulated in [7]:

$$\begin{cases} \ddot{x} + \varepsilon \kappa \dot{x} + (1 + \varepsilon \cos 2t)x + \varepsilon c y & = 0, \\ \ddot{y} - \varepsilon \mu (1 - y^2) \dot{y} + y + \varepsilon a y^3 + \varepsilon c x & = 0. \end{cases} \quad (16)$$

The system formulation is inspired by the work of A. Tondl, see [22]. We have weak linear interaction between the 2 oscillators governed by parameter  $c$ , with parameters



$\kappa, \mu, a$ . General position periodic solutions are candidates to produce tori by bifurcation. Without interaction ( $c = 0$ ), the equation for  $x(t)$  will have periodic solutions forced by the parametric  $\cos 2t$  term. The equation for  $y(t)$  without interaction will have periodic solutions with a period branching off the harmonic solution and will be close to  $2\pi$ . The parameter  $a$  is introduced as the Van der Pol- equation has a  $2\pi$ -periodic solution in an  $O(\varepsilon)$  approximation, if  $a = 0$  one needs higher order approximations as a change of the period  $2\pi$  arises at  $O(\varepsilon^2)$ .

### 3.1 Periodic solutions by averaging

We use the transformations  $x, \dot{x} \mapsto r, \dot{\phi}$  and  $y, \dot{y} \mapsto R, \dot{\psi}$ :

$$x(t) = r(t) \cos(t + \phi(t)), \dot{x}(t) = -r(t) \sin(t + \phi(t)),$$

$$y(t) = R(t) \cos(t + \psi(t)), \dot{y}(t) = -R(t) \sin(t + \psi(t)).$$

Transforming produces slowly variational equations for the positive amplitudes  $r, R$  and phases  $\phi, \psi$ . We leave out the variational equations. After averaging over time we find:

$$\begin{cases} \dot{r} &= \frac{\varepsilon}{2}(-\kappa r + \frac{1}{2}r \sin 2\phi + cR \sin \chi), \\ \dot{\phi} &= \frac{\varepsilon}{2r}(\frac{1}{2}r \cos 2\phi + cR \cos \chi), \\ \dot{R} &= \frac{\varepsilon}{2}(\mu R(1 - \frac{1}{4}R^2) - cr \sin \chi), \\ \dot{\psi} &= \varepsilon \frac{3a}{8}R^2 - \frac{\varepsilon}{2}c \frac{r}{R} \cos \chi, \end{cases} \quad (17)$$

with  $\chi = \phi - \psi$ . The solutions of system (17) produce  $O(\varepsilon)$  approximations of the solutions of system (16) valid on the timescale  $1/\varepsilon$ . The zeros of the righthand sides of system (17) with  $r, R \neq 0$  correspond with general position periodic solutions of system (16).

Eliminating  $\cos \chi$  and  $\sin \chi$  from the critical equations produces:

$$\cos 2\phi = -\frac{3}{2}a \frac{R^4}{r^2}, \quad \sin 2\phi = 2\kappa - 2\mu \frac{R^2}{r^2} \left(1 - \frac{1}{4}R^2\right). \quad (18)$$

We look for solutions with:

$$\cos 2\phi = \frac{1}{2}, \quad \sin 2\phi = \pm \frac{1}{2}\sqrt{3}. \quad (19)$$

Substitution for  $\cos \phi, \sin 2\phi$  in eq. (18) produces for  $a < 1$  the amplitudes given by:

$$r_c^2 = -3aR_c^4, \quad R_c^2 = \frac{2}{\pm \frac{3a}{\mu}\sqrt{3} - 12\frac{a\kappa}{\mu} + 1}. \quad (20)$$

Example:  $a = -1/3, \mu = 4$  gives  $r_c^2 = R_c^4 = 2/(\mp\sqrt{3}/4 + \kappa + 1)$ .

## 3.2 Neimark-Sacker bifurcation by averaging

### 3.3 Iteration for integral equations

In section 3.1 we have obtained periodic solutions by looking for critical points (equilibria) of the averaged system. Another, but related method is the Poincaré-Lindstedt method where one uses iteration of a corresponding integral equation while applying periodicity conditions. The iteration method was generalised in [26] by iteration, expansion with respect to the small parameter and applying secularity conditions. As the expansions produce approximations on the timescale  $O(1)$  the method does also apply to quasi-periodic solutions and families of them.

Considering system (16) we formulate 2 equivalent integral equations using amplitude-phase representations:

$$\begin{cases} x(t) &= r(t) \cos(t + \phi(t)) + \varepsilon \int_0^t \sin(t-s) [\kappa r(s) \sin s + \phi(s) - \\ &\cos 2s r(s) \cos(s + \phi(s)) - cR(s) \cos(s + \psi(s))] ds, \\ y(t) &= R(t) \cos(t + \psi(t)) + \varepsilon \int_0^t \sin(t-s) [-\mu(1 - R^2(s) \cos^2(s + \psi(s)) \\ &R(s) \sin(s + \psi(s)) - aR^3(s) \cos^3(s + \psi(s)) - cr(s) \cos(s + \phi(s))] ds. \end{cases} \quad (21)$$

One can obtain a convergent series for the solutions of system (21) by contraction. Start with the harmonic solutions  $x^1 = r_0 \cos(t + \phi_0)$ ,  $y^1 = R_0 \cos(t + \psi_0)$  and substitute the expressions in the integrals. After applying secularity conditions one obtains a second order approximation for  $x(t)$ ,  $y(t)$ . Repeating the iteration process improves the approximations and leads to a convergent series.

#### Sufficient conditions for bounded solutions

Expanding  $r(t) = r_0 + \varepsilon \dots$ ,  $\phi(t) = \phi_0 + \varepsilon \dots$ ,  $R(t) = R_0 + \varepsilon \dots$ ,  $\psi(t) = \psi_0 + \varepsilon \dots$  we have to  $O(\varepsilon)$  the secularity conditions from  $x(t)$ :

$$\begin{cases} \kappa r_0 \sin \phi_0 - \frac{1}{2} r_0 \cos \phi_0 - cR_0 \cos \psi_0 = 0, \\ \kappa r_0 \cos \phi_0 - \frac{1}{2} r_0 \sin \phi_0 + cR_0 \sin \psi_0 = 0. \end{cases} \quad (22)$$

Considering system (22) as an algebraic system for  $r$ ,  $R$ , we have nontrivial solutions if the determinant is singular and  $c \neq 0$  leading to:

$$\kappa \cos(\phi_0 - \psi_0) - \frac{1}{2} \cos(\phi_0 + \psi_0) = 0. \quad (23)$$

The phases  $\phi_0$ ,  $\psi_0$  have to satisfy (23) with  $0 \leq \kappa \leq \frac{1}{2}$ .

The first order secularity conditions from the equation for  $y(t)$  are:

$$\begin{cases} \mu(1 - \frac{1}{8} R_0^3 \sin \psi_0) + \frac{3a}{8} R_0^3 \cos \psi_0 + \frac{c}{2} r_0 \cos \phi_0 = 0, \\ -\mu(1 - \frac{1}{8} R_0^3 \cos \psi_0) + \frac{3a}{8} R_0^3 \sin \psi_0 + \frac{c}{2} r_0 \sin \phi_0 = 0. \end{cases} \quad (24)$$

Solutions  $r_0$ ,  $R_0$ ,  $\phi_0$ ,  $\psi_0$  of eqs (22), (24) produce  $O(\varepsilon)$  approximations of  $x(t)$ ,  $y(t)$  that are bounded.

### Necessary conditions for bounded solutions

In an amplitude-phase representation of the solutions of system (16) we can restrict ourselves to the requirement of boundedness of the amplitudes. The variational equations are:

$$\begin{cases} \dot{r} &= -\varepsilon \sin(t + \phi) [\kappa r \sin(t + \phi) - \frac{1}{2}r \cos(3t + \phi) - \frac{1}{2}r \cos(t - \phi) - cR \cos(t + \psi)], \\ \dot{R} &= \varepsilon \sin(t + \psi) [-\mu R \sin(t + \psi) + \frac{1}{2}\mu R^3 \sin(t + \psi) + \frac{1}{4}R^3 \sin(3t + 3\psi) - \\ &\frac{1}{4}\mu] R^3 \sin(t - \psi) - \frac{3}{4}aR^3 \cos(t + \psi) - \frac{1}{4}aR^3 \cos(3t + 3\psi) - cr \cos(t + \phi)]. \end{cases} \quad (25)$$

Putting  $\chi = \phi_0 - \psi_0$  we find when expanding to  $O(\varepsilon)$  the secularity conditions:

$$\begin{cases} cR_0 \sin \chi &= r_0(\kappa - \sin 2\phi_0), \\ cr_0 \sin \chi &= \mu R_0(1 - \frac{1}{2}R^2 + \frac{1}{4}R^2 \cos 2\psi_0). \end{cases} \quad (26)$$

The secularity conditions (26) lead to bounded solutions but not necessarily to periodic or quasi-periodic solutions; that would require conditions on the phases. The nontriviality condition (23) can be used to find suitable initial phases, for instance:

$$\kappa = \frac{1}{2}, \phi_0 = \psi_0 = \pm \frac{\pi}{4}.$$

## References

- [1] V.I. Arnold, V.V. Kozlov and A.I. Neihstadt, *Mathematical aspects of classical and celestial mechanics*, Encyclopaedia of Mathematical Sciences (V.I. Arnold, ed.), Dynamical Systems III, Springer (1988).
- [2] E. Doedel, A.R. Champneys, T.F. Fairgrieve, Yu.A. Kuznetsov, B. Sandstede, and X.J. Wang, *AUTO97: Continuation and bifurcation software for ordinary differential equations* (with Hom-Cont), Concordia University, Montreal, Canada, silver edition, 1997. Download versions at GifHub and SourceForge.
- [3] T. Bakri, R. Nabergoj, A. Tondl and F. Verhulst, *Parametric excitation in nonlinear dynamics*, Int. J. Nonlinear Mech. 39, pp. 311-329 (2004).
- [4] T. Bakri, R. Nabergoj, A. Tondl, *Multi-frequency oscillations in self-excited systems*, Nonlinear Dynamics, DOI 10.1007/s11071-006-9077-1 (2006).
- [5] Taoufik Bakri and Ferdinand Verhulst, *Bifurcations and quasi-periodic dynamics: torus breakdown*, Z. Angew. Math. Phys. 65, pp. 1053-1076 (2014).
- [6] T. Bakri, Y.A. Kuznetsov and F. Verhulst, *Torus bifurcations in a mechanical system*, J. Dyn. Diff. Equat. 27 pp. 371-403 (2015).

- [7] Taoufik Bakri and Ferdinand Verhulst, *From A. Tondl's Dutch contacts to Neimark-Sacker-bifurcation*, Appl. and Comp. Mechanics 16, pp. 87-100, doi.org/10.24132/acm.2022.770 (2022).
- [8] Taoufik Bakri and Ferdinand Verhulst, *Time-reversal, tori families and canards in the Sprott A and NE9 systems*, CHAOS doi: 10.1063/s.0097508 (August 2022).
- [9] M-C. Ciocci, A. Litvak-Hinenzon and H.W. Broer., *Survey on dissipative KAM theory including quasi-periodic bifurcation theory*, Geometric Mechanics and Symmetry: the Peyresq Lectures, 306, pp. 303-355 (2005).
- [10] S. Jafari, J.C. Sprott and S. Golpayegani, *Elementary quadratic chaotic flows with no equilibria*, Physics Letters A 377, pp. 699-702 (2013).
- [11] V.V. Kozlov, *Symmetries, Topology and Resonances in Hamiltonian Mechanics*, Springer (1995).
- [12] Yu.A. Kuznetsov, *Elements of applied bifurcation theory*, (rev. ed.) Springer (2004).
- [13] J.S.W. Lamb and J.A.G. Roberts, *Time-reversal symmetry in dynamical systems: A survey*, Physica D 112, pp. 61-39702 (1998).
- [14] J. Laskar. Frequency analysis of a dynamical system. Celestial Mechanics and Dynamical Astronomy 56, pp. 191–196, (1993).
- [15] MATCONT, Numerical continuation and bifurcation program, available at <http://www.matcont.ugent.be>
- [16] M. Messias and A.C. Reinol, *On the formation of hidden chaotic attractors and nested invariant tori in the Sprott A system*, Nonlinear Dyn. 88, pp.807-821 (2017).
- [17] M. Messias and A.C. Reinol, *On the existence of periodic orbits and KAM tori in the Sprott A system: a special case of the Nosé-Hoover oscillator*, Nonlinear Dyn. 92, pp. 1287-1297 (2018).
- [18] J.A.G. Roberts and G.R.W. Quispel *Chaos and time-reversal symmetry. Order and chaos in reversible dynamical systems*, Physics Reports 216, pp. 63-177 (1992).
- [19] J.A. Sanders, F. Verhulst, F. and J. Murdock, *Averaging methods in nonlinear dynamical systems*, rev.ed. Springer-Verlag (2007).
- [20] J.C. Sprott, *Some simple chaotic flows*, Physical Review E 50, pp. R647-R650 (1994).
- [21] A.N. Tikhonov, *Systems of differential equations containing a small parameter multiplying the derivative* (in Russian), Math. Sb. 31 (73), 575-586 (1952).

- [22] A. Tondl, *On the interaction between self-excited and parametric vibrations*, National Research Institute for Machine Design, Běchovice, Monographs and Memoranda 25, Prague (1978).
- [23] A. Tondl, M. Ruijgrok, F. Verhulst and R. Nabergoj, *Autoparametric resonance in mechanical systems*, Cambridge University Press, 196 pp. (2000).
- [24] Ferdinand Verhulst, *Nonlinear differential equations and dynamical systems* 2nd ed., Springer, New York etc., (2000).
- [25] Ferdinand Verhulst, *Methods and applications of singular perturbations*, Springer, New York etc., (2005).
- [26] Ferdinand Verhulst, *A Toolbox of Averaging Theorems, ordinary and partial differential equations*, Surveys and Tutorials in the Applied Mathematical Sciences, Springer (2023).